

FAILURE ANALYSIS OF AN EYEBAR

J.A.O.F. DUARTE, F.M.F. OLIVEIRA, P.M.S.T. DE CASTRO*

The present paper reports a failure analysis conducted on an eyebar of a heavy wood cutting machine. The engineering approximations and assumptions are described. Numerical and experimental stress analysis and materials testing, including fatigue crack growth testing were used, together with a fractographic examination using a scanning electron microscope. Results of the analysis, particularly the satisfactory agreement between estimated and actual service life are discussed. The actions taken to preclude fracture in service are presented.

INTRODUCTION

As a result of important research efforts into the fracture of solids on disciplines such as stress analysis, materials science, nondestructive examination, etc., many problems of the mechanics of fracture are now well understood. Research papers and reviews of this research are found in the many technical journals associated with the various relevant specialities. Applications of this knowledge are not, however, easily found documented in papers. This situation is identified by Rich and Cartwright (1), editors of a very useful compilation of case studies. Presenting this work, they state the need for papers documenting results of applications experience, in order that the incorporation of fracture mechanics into actual engineering problems can become more effective. The present paper described such a failure examination, conducted on an eyebar of a wood cutting machine.

A good design should ensure that fractures will not occur during the service life of the component. Traditionally, the use of safety factors seeks to overcome the difficulties of accurately predicting all the possible circumstances which may lead to a reduction of the expected service life. Among the phenomena responsible for these premature failures, initiation and growth of a fatigue crack, stress corrosion cracking, and local defects can be mentioned. As far as fatigue is concerned,

*Oporto University, Faculty of Engineering, Rua dos Bragas, 4099 Oporto, Portugal.

it is well known that a fatigue crack initiated from a small defect propagates in a stable manner under nominal stresses within the limits accepted as safe, until it reaches a critical size at which catastrophic failure occurs.

Fracture mechanics make it possible to predict the fatigue crack growth rate and the service life of the component. Design criteria can aim at finite or infinite life. The first criterion requires knowledge of the crack growth behaviour, as well as of the critical crack length for final catastrophic failure, either by brittle fracture or by plastic collapse. A complete stress analysis, including appropriate stress intensity factor calibrations are also required. As far as infinite life design is concerned, the main material property required is the threshold value of the stress intensity factor ΔK_{th} , below which crack growth will not occur.

BACKGROUND OF THE PROBLEM

The failed eyebar is part of a machine for cutting wood sheets from 4.5 meter-long logs, with a typical width of 0.7m. The main geometric details of the crank-connecting rod mechanism which includes the failed eyebar are presented in Figure 1. The large size of the machine is suggested by stating that the blade and associated parts subjected to alternating linear movement have an estimated mass greater than 7,000 Kg. The movement of this alternating body is imposed by two parallel mechanisms of the type shown in Figure 1. Maximum working speed, commonly used, is 60 cycles per minute, suggesting the high inertial forces present and the importance of the structural integrity of the eyebar, object of the present study.

Catastrophic failure of the eyebar occurred suddenly during service, the crack developing in the direction shown in Figure 1b, starting at the outside of the component. The operator noticed no abnormality until sudden fracture took place. The broken part was later subjected to a failure examination, as reported hereafter.

FORMULATION OF THE FAILURE ANALYSIS

The investigation to determine possible mechanisms for fracture was carried out using a number of experimental and analytical techniques. Firstly, the chemical composition of the cast steel was determined using spectrometry; conventional tensile and hardness tests were carried out. The service conditions suggested very strongly the occurrence of a fatigue mechanism, the crack propagating under cyclic loading up to a given critical length. However, macroscopic observation of the fracture surface was rather inconclusive. Scanning electron microscopy was used to make a detailed examination of the fracture surface. If the problem was indeed a fatigue crack growth situation, then an adequate stress analysis was required, firstly to know the actual load axially transmitted by the connecting rod, and then, for this force, the stress distribution in the eyebar, particularly the stress concentration in the connection eyebar-connecting rod. The machine being already repaired at the time this analysis was carried out, and working seven days per week on a heavy schedule, it was not possible to measure the mass of

the moving parts, and therefore the force transmitted was measured in service using extensometry.

ASSESSMENT

The chemical composition of the cast steel, obtained by spectrometry, is given in Table 1.

TABLE 1 - Chemical Composition of Cast Steel

| | C | Mn | P | S | Si | Cu | Cr | Ni | Mo | Sn | Al |
|---|-----|-----|------|------|-----|------|------|------|------|------|------|
| % | .20 | .78 | .014 | .020 | .32 | .249 | .208 | .117 | .020 | .029 | .025 |

Tensile testing, according to DIN 50145, and hardness testing, according to DIN 50351, were carried out and gave the results presented in Table 2.

TABLE 2 - Conventional Mechanical Data

| | |
|---------------------------|------------------------------------|
| Yield stress | $\sigma_Y = 275 \text{ Nmm}^{-2}$ |
| Ultimate stress | $\sigma_U = 457 \text{ Nmm}^{-2}$ |
| Elongation | $\epsilon_f = 13.5\%$ |
| Hardness 30D ² | 153 HB ⁺⁹ ₋₄ |

The data obtained indicate an unexpectedly low value of ϵ_f , together with a great scatter of hardness values which suggests a highly heterogeneous material.

Scanning electron microscopy was then conducted on the fracture surface of the failed eyebar. This examination revealed clearly that the component failed by fatigue, striations being found in the crack path, starting from the stress concentration shown in Figure 1b up to final fracture, showing typical void coalescence, i.e., a ductile final fracture. Typical observations are shown in Figures 2a-2d. Figure 2a shows a typical view of fatigue striations; this behaviour is documented by using a higher amplification, in Figure 2b. Figure 2c shows a typical inclusion, whereas Figure 2d describes final fracture appearance.

The s.e.m. examination identified several very important facts: firstly, the failure consisted of fatigue crack propagation from an initial defect in the region of high stress concentration, Figure 2b. Secondly, the material has a large number of pores and inclusions similar to the one shown in Figure 2c. These were found, using X-ray dispersion analysis, to be SMn inclusions.

The failure analysis requires the knowledge of the crack growth behaviour of the material. Testing was conducted on a compact tension geometry, CT specimens being machined from the failed component. Testing was carried out at room temperature, in a servohydraulic MTS fatigue testing machine of 250 kN capacity, at 10 Hz, under constant load cycling, R = 0.1. The a versus 'N' plot was used to derive the da/dN versus ΔK data.

The stress intensity factor K is given in ASTM E647, and da/dN data was obtained graphically. The resulting data is presented in Figure 3. Values of C and m in the Paris relationship

$$da/dN = C(\Delta K_I)^m$$

were found to be $C = 7.94 \times 10^{-18}$ and $m = 4.6$, for da/dN expressed in mm/cycle and ΔK in $Nmm^{-3/2}$.

The next item dealt with is the stress analysis of the part. This was carried out using extensometry to identify the axial load transmitted by the connecting rod under service conditions. At 60 cycles per minute, the axial load was 192 KN, giving for the connecting rod of cross section 4440 mm² an axial maximum normal stress per cycle of 43 Nmm⁻². The stress distribution in the crack plane results from the superposition of traction and bending loading. Blake (2), for the connecting rod axial load of interest, gives in this plane, a traction of 68 KN and a bending moment of 1.90 MNmm. From these loadings, the nominal stress distribution is easily obtained. However, to identify stress concentration effects, a finite element analysis was carried out. The computer code uses 8-node isoparametric elements, and is described by Hinton and Owen (3). The mesh is described in Figure 4, where the region of crack propagation is shown enlarged. Finite element computations gave the stress concentration effect (point A in Figure 4) comparing the computed stress levels with the nominal values previously obtained. The present stress analysis was confirmed by a photoelastic examination, of which Figure 5 shows the model and fringe pattern.

FATIGUE CRACK GROWTH ANALYSIS AND DISCUSSION

The initial defect size was estimated using the ΔK_{th} given in (4), i.e. $\Delta K_{th} = 190 Nmm^{-3/2}$. The stress intensity factor solution was estimated as

$$K_I = SCF (K_{It} + K_{Ib})$$

where SCF is the stress concentration factor; K_{It} corresponds to traction loading and K_{Ib} to bending loading, from Rooke and Cartwright (5). From $\Delta K_{th} = SCF (K_{It} + K_{Ib})$, the value of initial crack depth was found to be $a_i = 0.763$ mm. The analysis was conducted assuming the crack to be a long crack of depth a , i.e., the possible semi-elliptic shape was not taken into account. This was supported by the s.e.m. examination, and implies a maximum value for K_I .

As a result of the s.e.m. study, the region of final fracture was found to correspond to a final ligament estimated as 12 mm, i.e., $a_f = 52 - 12 = 40$ mm. Fatigue crack propagation occurs from a_i to a_f . This interval was divided into six smaller intervals of 6.5 mm in length. K_I was obtained for the mean crack length of each interval. Nominal K_I value (the sum $K_{It} + K_{Ib}$) was multiplied by the value of SCF corresponding to the point of interest, to take into account the effect of the stress concentration (maximum at the surface, and decreasing towards SCF = 1). Corresponding values of da/dN were obtained from Figure 3. These da/dN values were then used to estimate

the number of cycles corresponding to each interval. The analysis is summarized in Table 3.

TABLE 3 - Fatigue Crack Growth Analysis

| a mm | SCF | a/b | K_I $Nmm^{-3/2}$ | da/dN mm/cycle | N |
|---------|-------|--------|-----------------------|-----------------------|--------------------|
| 4 | 1.6 | 0.0769 | 272.54 | 6.16×10^{-7} | 1.05×10^7 |
| 10.5 | 1.5 | 0.2019 | 418.3 | 5.12×10^{-6} | 1.26×10^6 |
| 17 | 1.075 | 0.3269 | 413.71 | 4.26×10^{-6} | 1.52×10^6 |
| 23.5 | 1 | 0.4519 | 520.34 | 1.12×10^{-5} | 5.80×10^5 |
| 30 | 1 | 0.5769 | 753.13 | 6.6×10^{-5} | 9.8×10^4 |
| 36.5 | 1 | 0.7019 | 1431.6 | 1.5×10^{-3} | 4.33×10^3 |

$$\Delta a = 6.5 \text{ mm}; b = 52 \text{ mm}$$

The analysis gives an estimated service life of $N = 1.39 \times 10^7$ cycles, rather close to the actual service life of the component, estimated as approximately 10^7 cycles.

The present analysis includes several assumptions, namely the shape of the initial crack, taken to be a long crack, the K_I calibration estimated as being given by the SCF multiplied by the nominal K (value of K corresponding to nominal σ), and the final crack length a_f . The final crack length observed in s.e.m. was not regular, and a_f was taken as a typical value. However, for the calculation of number of cycles during service life, a_f is not an important parameter, assumptions relating to a_i being far more important. The close agreement between estimated number of cycles and actual service life, indicates however that the assumptions made were reasonable.

The failed part was replaced by an eyebar made of a better steel, with no pores present. It was obvious that failure resulted from the poor quality of the original material, particularly the large amount of pores and large inclusions of rather irregular shape. Additionally, the geometry of the eyebar in the critical region was modified to give lower values of stress.

The present paper seeks to present an example of how materials testing, scanning electron microscopy, and numerical and experimental stress analysis can be combined to give adequate interpretations of actual fracture problems.

CONCLUSIONS

- Reasons for failure of an important machine element were examined and traced to the use of an inadequate cast steel.
- The engineering assumptions and approximations made are described and assessed.
- Fatigue crack growth data for a cast steel is presented.

SYMBOLS

- a - crack length
- b - width
- C - Paris law constant
- K_I - stress intensity factor, Mode I
- K_{It} - traction loading K_I
- K_{Ib} - bending loading K_I
- N - number of cycles
- R - min. load/max. load ratio
- s.e.m. - scanning electron microscopy
- SCF - Stress Concentration Factor
- σ - stress
- ϵ - elongation

REFERENCES

1. Rich, T.P., and Cartwright, D.J., eds., "Case Studies in Fracture Mechanics", (U.S. Army Materials and Mechanics Research Center, report AMMRC MS 77-5, June 1977).
2. Blake, A., "Practical Stress Analysis in Engineering Design", (Marcel Dekker, 1982).
3. Hinton, E., and Owen, D.R.J., "Finite Element Programming", (Academic Press, London, 1977).
4. British Standards Institution, "Guidance on Some Methods for the Derivation of Acceptance Levels for Defects in Fusion Welded Joints", (BS PD 6493, 1980).
5. Rooke, D.P., and Cartwright, D.J., "Compendium of Stress Intensity Factors", (Her Majesty's Stationery Office, London, 1976).

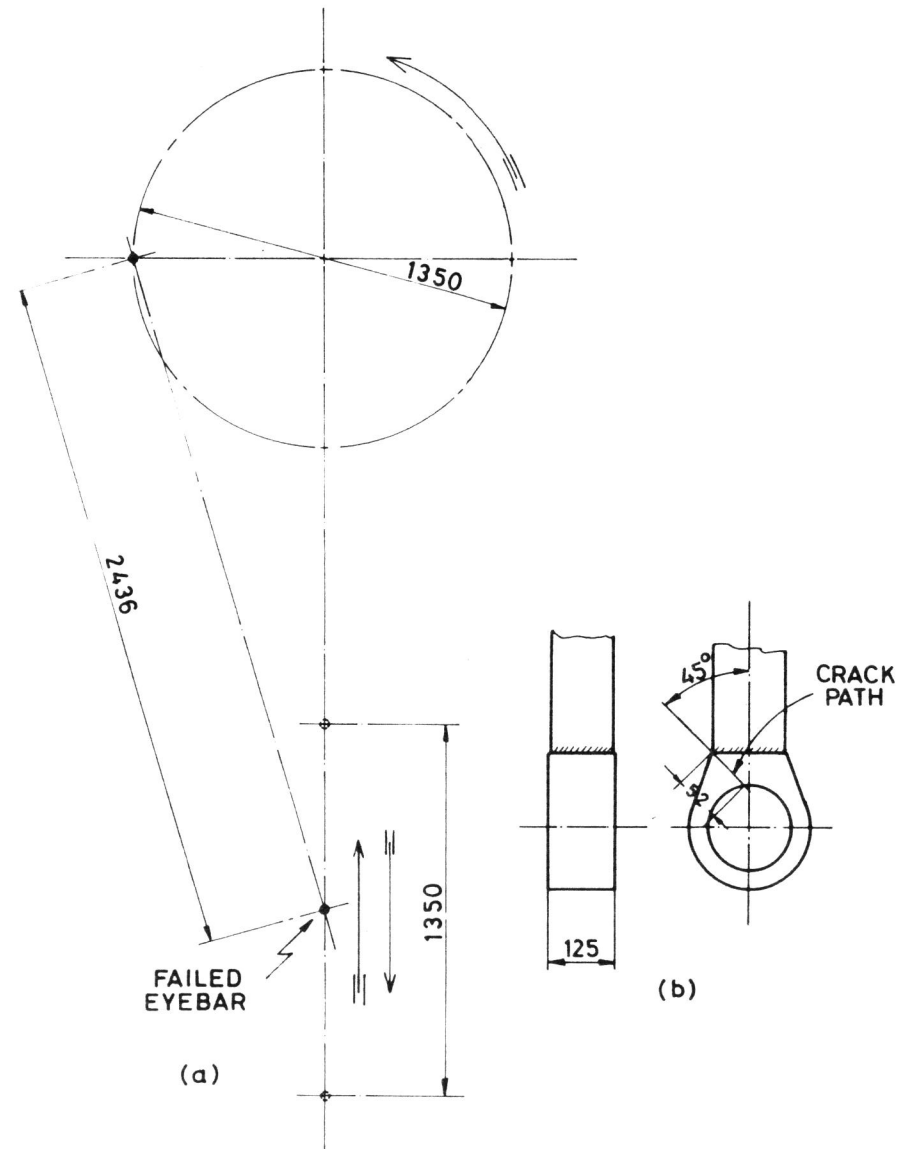
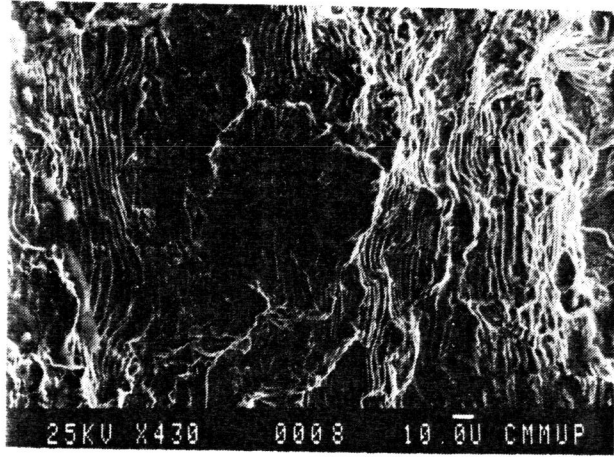
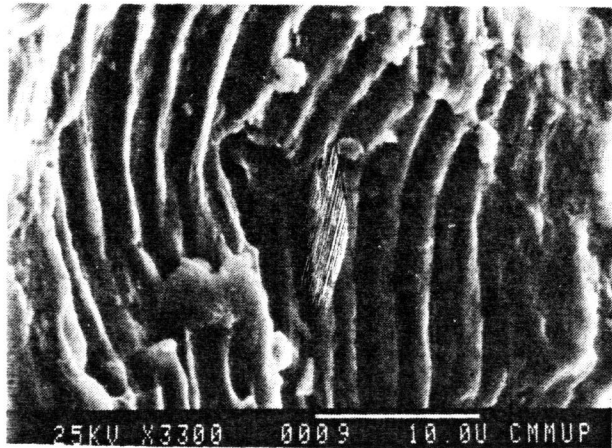


Figure 1, (a) - crank - connecting rod mechanism; (b) - eyebar

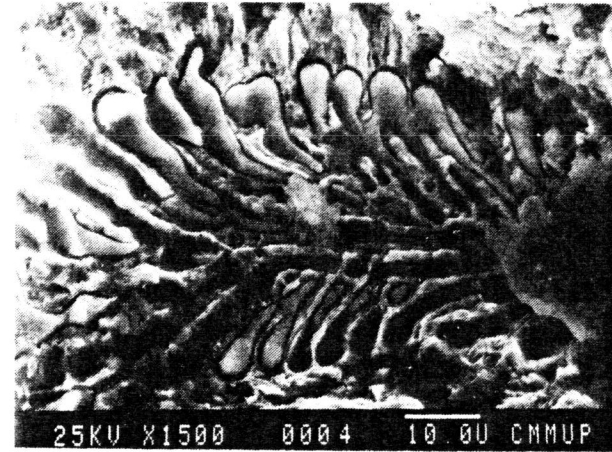


(a)

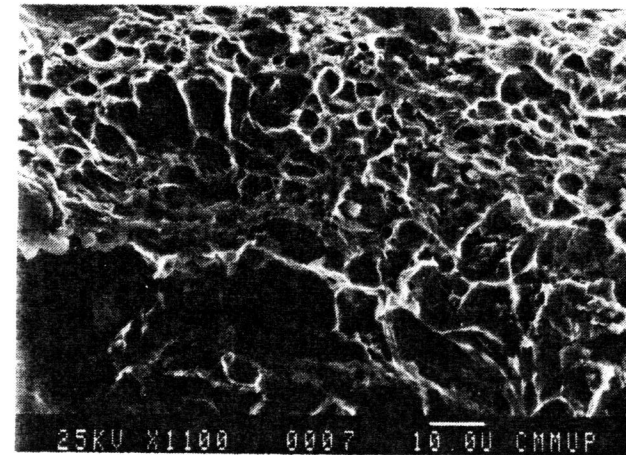


(b)

Figure 2, (a) - fatigue striations; (b) - fatigue striations, using a higher amplification



(c)



(d)

Figure 2, (c) - typical inclusion, SMn; (d) - final fracture

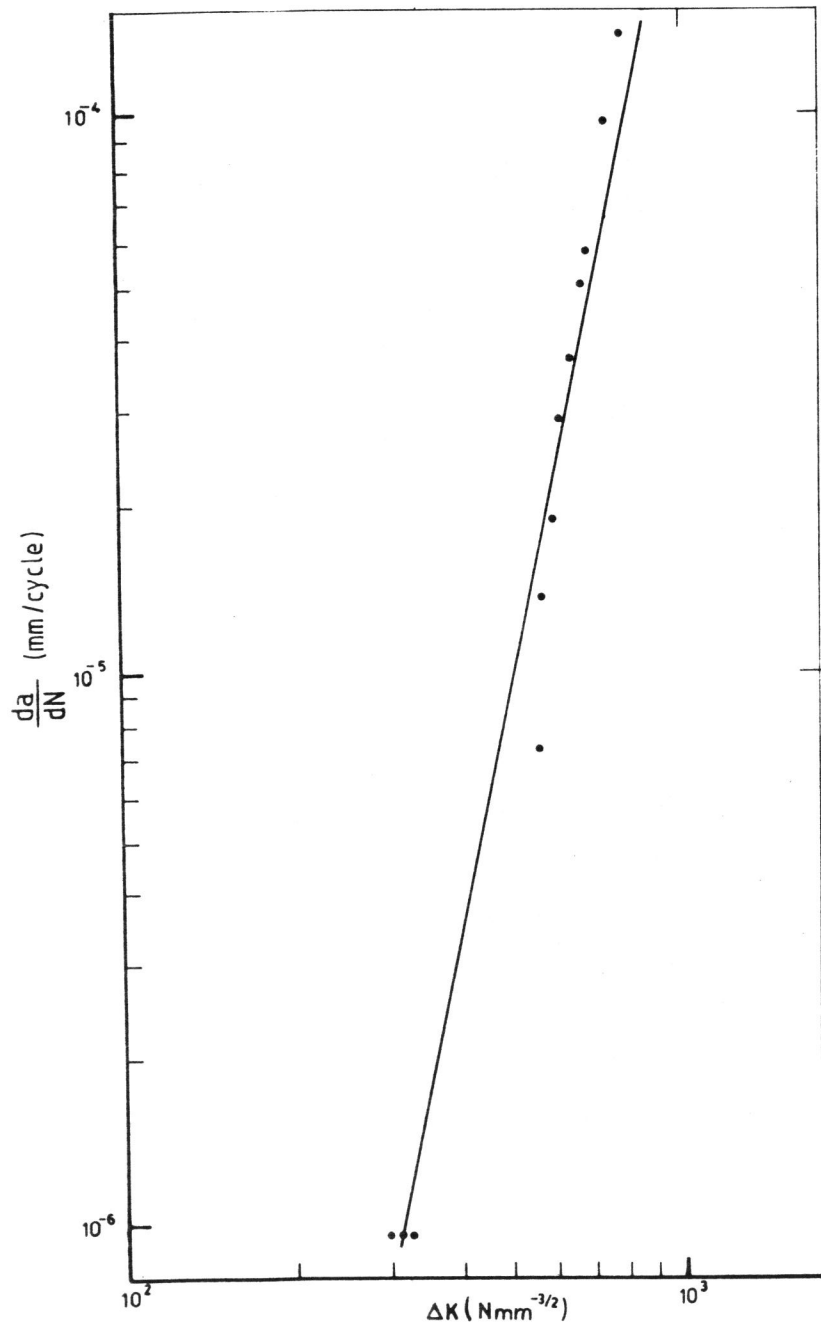


Figure 3 - da/dN versus ΔK data for the cast steel

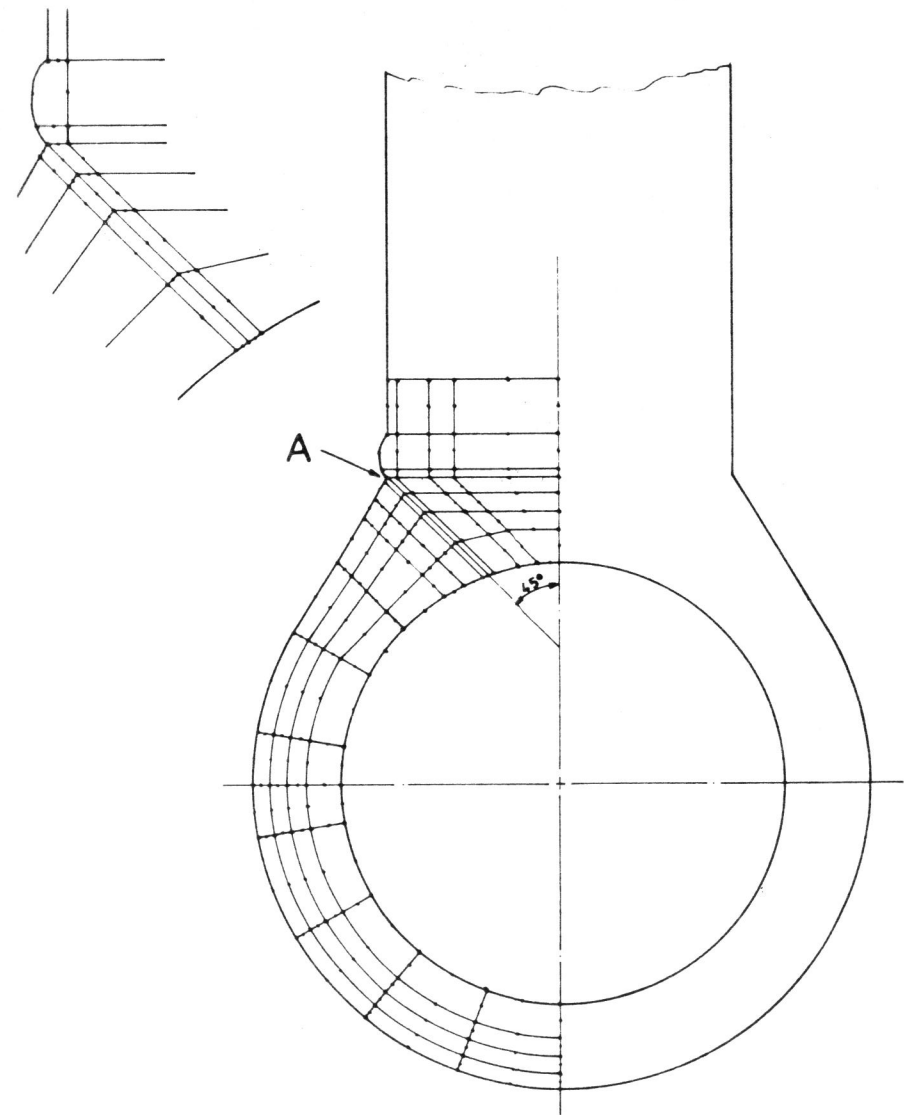


Figure 4 - finite element mesh

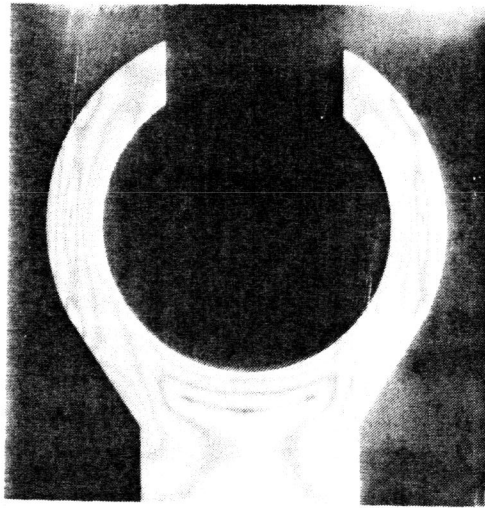


Figure 5 - photoelastic model of the eyebar

